

## GRBs on probation: testing the UHE CR paradigm with IceCube

M. Ahlers<sup>a</sup>, M. C. Gonzalez-Garcia<sup>a,b</sup>, F. Halzen<sup>c</sup><sup>a</sup>*C.N. Yang Institute for Theoretical Physics, SUNY at Stony Brook, Stony Brook, NY 11794-3840, USA*<sup>b</sup>*Institució Catalana de Recerca i Estudis Avançats (ICREA), Departament d'Estructura i Constituents de la Matèria and ICC-UB, Universitat de Barcelona, 647 Diagonal, E-08028 Barcelona, Spain*<sup>c</sup>*Department of Physics, University of Wisconsin, Madison, WI 53706, USA*

---

**Abstract**

Gamma ray burst (GRB) fireballs provide one of very few astrophysical environments where one can contemplate the acceleration of cosmic rays to energies that exceed  $10^{20}$  eV. The assumption that GRBs are the sources of the observed cosmic rays generates a calculable flux of neutrinos produced when the protons interact with fireball photons. With data taken during construction IceCube has already reached a sensitivity to observe neutrinos produced in temporal coincidence with individual GRBs provided that they are the sources of the observed extra-galactic cosmic rays. We here point out that the GRB origin of cosmic rays is also challenged by the IceCube upper limit on a possible diffuse flux of cosmic neutrinos which should not be exceeded by the flux produced by all GRB over Hubble time. Our alternative approach has the advantage of directly relating the diffuse flux produced by all GRBs to measurements of the cosmic ray flux. It also generates both the neutrino flux produced by the sources and the associated cosmogenic neutrino flux in a synergetic way.

*Keywords:* gamma ray burst, cosmogenic neutrinos

---

**1. Motivation**

There is compelling evidence that the collapse of a massive star to a black hole is the primary engine of long-duration Gamma Ray Bursts (GRBs). The phenomenology that successfully accommodates the astronomical observations is that of the creation of a hot fireball of electrons, photons and protons that is initially opaque to radiation. The hot plasma therefore expands by radiation pressure and particles are accelerated to a Lorentz factor  $\Gamma$  that grows until the plasma becomes optically thin and produces the GRB display. From this point the fireball is coasting with a Lorentz factor that is constant and depends on its baryonic load. The baryonic component carries the bulk of the fireball's kinetic energy. The energetics and rapid time structure of the burst can be successfully explained by shocks generated in the expanding fireball [1–3]. Here, the temporal variation of the  $\gamma$ -ray burst of the order of milliseconds can be interpreted as the collision of internal shocks with a varying baryonic load leading to differences in the bulk Lorentz factor. Electrons accelerated by first order Fermi acceleration radiate synchrotron  $\gamma$ -rays in the strong internal magnetic field and thus produce spikes in the burst spectra of the order of seconds [4, 5]. The collision of the fireball with interstellar gas forms external shocks that can explain the GRB afterglow ranging from X-ray to the optical [6, 7]. (See also [8] for a recent review on theoretical models.)

---

*Email addresses:* [ahlers@insti.physics.sunysb.edu](mailto:ahlers@insti.physics.sunysb.edu) (M. Ahlers), [concha@insti.physics.sunysb.edu](mailto:concha@insti.physics.sunysb.edu) (M. C. Gonzalez-Garcia), [halzen@icecube.wisc.edu](mailto:halzen@icecube.wisc.edu) (F. Halzen)

It has been pointed out that fireball baryons may be the source of ultra-high energy (UHE) cosmic rays (CRs) with energies extending to at least  $3 \times 10^{20}$  eV. Baryons are inevitably accelerated along with the electrons in the expanding fireball with their energies boosted by the bulk Lorentz factor. It has been shown that a typical GRB environment can naturally satisfy the requirements to produce UHE CRs, most likely protons. It is not easy to conceive of a mechanism where nuclei survive acceleration in a GRB fireball environment. (Heavy nuclei could be synthesized in magnetically-dominated jets as in the proto-magnetar model of GRBs, see *e.g.* [9].) The results of CR observatories disagree with HiRes [10] claiming protons and Auger [11] heavier primaries. These conflicting results may just illustrate that, given the poor knowledge of hadronic interactions more than one order of magnitude above LHC energies, is not sufficiently known to derive a definite result [12].

Though GRBs satisfy the necessary conditions for accelerating protons to UHE, it is problematic how these protons may eventually be ejected as CRs: protons are magnetically confined to the expanding fireball and its adiabatic cooling will reduce the maximum proton energy significantly [13, 14]. However, this does not concern neutrons that are frequently produced in  $p\gamma$ -interactions of accelerated protons with fireball photons by processes like  $p\gamma \rightarrow \Delta^+ \rightarrow n\pi^+$ . Cosmic ray protons could thus be identified as neutrons from  $p\gamma$ -interactions that can escape from the magnetic environment and  $\beta$ -decay back to protons at a safe distance. A smoking-gun test of this scenario is the production of PeV neutrinos from the decay of the charged pions inevitably produced along with the neutrons [15–18]. This neutrino flux is in reach of large-scale neutrino telescopes like IceCube [19, 20]. (Possible emission of neutrinos associated to the GRB progenitor and prior to the  $\gamma$ -ray burst have been discussed in [21]. Neutrinos from proton interactions in late internal or external shocks during the afterglow phase have been considered in [22–24].)

In this paper we calculate the diffuse flux of neutrinos produced in association with GRB cosmic rays by directly fitting the proton spectra from the decay of fireball neutrons to CR data from HiRes. As a byproduct we also obtain the flux of so-called GZK neutrinos produced when the cosmic rays interact with microwave and infra-red/optical background photons [25, 26]. The accompanying photon flux resulting from the electromagnetic cascading of the neutral pions peaks in the MeV-GeV energy region; we verify that it does not exceed the extra-galactic diffuse  $\gamma$ -ray flux inferred by Fermi-LAT [27]. Our main conclusion is that the predicted flux exceeds the upper bound on a diffuse flux of cosmic neutrinos obtained by IceCube from a year of data taken with half the instrument during construction. Facing this negative conclusion, we subsequently investigate the dependence of the predicted neutrino flux on the cosmological evolution of the sources as well as on the parameters describing the fireball. Although the latter are constrained by the electromagnetic observation as well as by the requirement that the fireball must accommodate the observed cosmic ray spectrum, the predictions can be stretched to the point that it will take 3 years of data with the now completed instrument to conclusively rule out the GRB origin of UHE CRs.

We work throughout in natural Heaviside-Lorentz units with  $\hbar = c = \epsilon_0 = \mu_0 = 1$ ,  $\alpha = e^2/(4\pi) \simeq 1/137$  and  $1 \text{ G} \simeq 1.95 \times 10^{-2} \text{ eV}^2$ .

## 2. Fireball Model

In the fireball model the GRB central engine produces a heated optically thick plasma of leptons, photons and baryons which is initially at rest. The fireball expands adiabatically by radiation pressure until it becomes optically thin. From this point on the fireball is coasting with a Lorentz factor  $\Gamma$  which depends on its baryonic load. The expanding plasma flow is shocked producing shells with varying baryonic load; this results in internal shells with different velocities that in their collision produce internal shocks. Although in the baryon-rich fireballs that would produce EHE cosmic rays most of the kinetic energy of the fireball is carried by the baryons, the internal shocks will convert a fraction  $\varepsilon_e = U'_e/U'_{\text{kin}}$  to leptons and  $\varepsilon_B = U'_B/U'_{\text{kin}}$  to magnetic fields supported by the plasma. Here and in the following, primed quantities refer to values in the comoving plasma frame, whereas unprimed quantities are reserved for the observer’s frame.

Study of the emission of GRB has resulted in “benchmark” parameters describing GRB fireball with the efficiency for lepton acceleration from bulk energy taken to be 10%, *i.e.*  $\varepsilon_e = 0.1$ . The fraction of magnetic field energy and hence the value of the turbulent magnetic field strength can be inferred from the observed peak of the  $\gamma$ -ray synchrotron spectrum with  $\varepsilon_B = 0.1$ , corresponding to equipartition of energy

in leptons and magnetic field. The “benchmark” parameters are required to produce the observed peak emission at MeV energies resulting from the synchrotron radiation of GRB electrons and must be consistent with afterglow observations. The typical radius of an internal shock  $r_i$  is given by the speed-of-light distance implied by the duration of the spikes observed in the GRB display. Because the shells are boosted toward the observer by a Lorentz factor  $\Gamma_i$ ,  $r_i \simeq t_v/(1 - \beta_i) \simeq 2\Gamma_i^2 t_v$ . We will take the variability scale to be  $t_v = 0.01$  s. Although variations in GRB spectra down to milliseconds have been observed, what is important here is the Fourier strength on the variability, and the choice can be debated. In any case, when obtaining our final results we will return to this problem and vary this as well as other critical benchmark parameters over a wide range.

Long-duration GRB are beamed; their observed isotropically-equivalent  $\gamma$ -ray luminosity is on average  $L_\gamma = 10^{52}$  erg/s. In the fireball model it results from synchrotron radiation by electrons accelerated in internal shocks. The spectral photon density of the burst ( $\text{GeV}^{-1} \text{cm}^{-3}$ ) in the observer’s frame can be adequately parametrized as [28]

$$n_\gamma \propto \begin{cases} (\epsilon/\epsilon_0)^\alpha e^{-\epsilon/\epsilon_0} & \epsilon < (\alpha - \beta)\epsilon_0 \\ (\alpha - \beta)^{\alpha - \beta} e^{\beta - \alpha} (\epsilon/\epsilon_0)^\beta & \epsilon > (\alpha - \beta)\epsilon_0 \end{cases} \quad (1)$$

with  $\alpha \simeq -1$ ,  $\beta \simeq -2.2$  and  $\epsilon_0 \simeq 1$  MeV. The normalization is given by  $U_\gamma = \int d\epsilon \epsilon n_\gamma(\epsilon) = L_\gamma/4\pi r_i^2$ . The corresponding photon density in the comoving frame is then given by  $n'_\gamma(\epsilon') = n_\gamma(\Gamma_i \epsilon')$ .

After Fermi acceleration the electron population follows a power-law spectrum with minimum energy  $E'_{e,\min} \simeq (\epsilon_e/\zeta_e)m_p$  in the comoving frame. Here  $\zeta_e < 1$  is the fraction of electrons that achieve equipartition [8]. This spectrum yields by synchrotron radiation a photon spectrum peaking at

$$\epsilon_0 \simeq \Gamma_i \frac{3}{2} \frac{eB'}{m_e^3} \left( \frac{\epsilon_e}{\zeta_e} m_p \right)^2 \simeq 0.8 \left( \frac{\epsilon_{e,-1}^3 \epsilon_{B,-1} L_{\gamma,52}}{\zeta_{e,-1}^4 \Gamma_{i,2.5}^4 t_{v,-2}^2} \right)^{1/2} \text{ MeV}, \quad (2)$$

where  $L_\gamma = L_{\gamma,52} 10^{52}$  erg/s,  $\epsilon_B = \epsilon_{B,-1} 0.1$ ,  $\epsilon_e = \epsilon_{e,-1} 0.1$ ,  $\zeta_e = \zeta_{e,-1} 0.1$ ,  $\Gamma_i = \Gamma_{i,2.5} 10^{2.5}$  and  $t_{v,-2} = t_{v,-2} 0.01$  s. This is close to the observed peak of the GRB burst spectrum at  $\mathcal{O}(\text{MeV})$ .

This concludes our description of the GRB fireball and its electromagnetic spectrum. There is nothing new here. We will next discuss the production of cosmic rays and neutrinos by applying the fireball phenomenology just described.

### 3. Cosmic Ray and Neutrino Emission

Although it is straightforward to argue that GRB fireballs represent an environment that can yield CRs of very high energy, it is important to take into account that the acceleration competes against energy loss due to synchrotron radiation and pion production. In other words, the fireball phenomenology is subject to the conditions that (i) the time to accelerate protons to the highest energy does not exceed the lifetime of the fireball and (ii) that the energy gained is not lost to synchrotron radiation and pion production. We discuss these constraints sequentially.

For efficient acceleration of UHE CR protons their gyroradius must be contained within the acceleration region which is related to the size of the shock. In the comoving frame the Larmor radius of a proton is  $r'_L = E'/eB'$  and the corresponding acceleration time  $c/r'_L$  is given by  $t'_{\text{acc}} = \eta r'_L$  with  $\eta \gtrsim 1$  or

$$t'_{\text{acc}} \simeq 8 \times 10^{10} \left( \frac{\eta^2 \epsilon_{e,-1} E_{p,20.5}^2 t_{v,-2}^2 \Gamma_{i,2.5}^4}{\epsilon_{B,-1} L_{\gamma,52}} \right)^{1/2} \text{ cm}, \quad (3)$$

where  $E_p = E_{p,20.5} 10^{20.5}$  eV, corresponding to the upper end of the UHE CR spectrum. The size of the accelerator is set by the size of the shock,  $t'_{\text{dyn}} \simeq r_i/2\Gamma_i = t_v \Gamma_i$ , or

$$t'_{\text{dyn}} \simeq 1 \times 10^{11} \Gamma_{i,2.5} t_{v,-2} \text{ cm}. \quad (4)$$

From this we derive the maximal proton energy in the observer's frame for which  $t'_{\text{dyn}} = t'_{\text{acc}}$ ,

$$E_{p,\text{max}} \simeq 4 \times 10^{20} \left( \frac{\varepsilon_{B,-1} L_{\gamma,52}}{\eta^2 \varepsilon_{e,-1} \Gamma_{i,2.5}^2} \right)^{1/2} \text{ eV} \quad (5)$$

We next consider the energy losses that compete with the acceleration. In the comoving frame the time scale associated with synchrotron radiation is  $t'_{\text{sync}} = 9\pi m^4 / E' e^4 B'^2$  or

$$t'_{\text{sync}} \simeq 7 \times 10^{10} \left( \frac{\varepsilon_{e,-1} \Gamma_{i,2.5}^7 t_{v,-2}^2}{\varepsilon_{B,-1} E_{p,20.5} L_{\gamma,52}} \right) \text{ cm} . \quad (6)$$

The maximal proton energy is reduced when  $t'_{\text{syn}} = t'_{\text{acc}}$  or is smaller; in this case, using (5)

$$E_{p,\text{max}} \simeq 3 \times 10^{20} \left( \frac{\varepsilon_{e,-1} \Gamma_{i,2.5}^{10} t_{v,-2}^2}{\eta^2 \varepsilon_{B,-1} L_{\gamma,52}} \right)^{1/4} \text{ eV} . \quad (7)$$

The photo-pion energy loss rate is determined by the  $p\gamma$  cross section, the photon density  $n_\gamma$  and the average energy loss of the protons  $\langle x_{p\gamma} \rangle$  in each interaction. In the  $\Delta^+$ -resonance approximation

$$t'_{\Delta^+}{}^{-1} \simeq \sigma_{\Delta} \langle x_{p \rightarrow \Delta^+} \rangle \Gamma_{\Delta^+} + \frac{\pi}{2} \frac{m_p}{E'_p} n_\gamma \left( \frac{\Gamma_i m_{\Delta^+}^2}{4E'_p} \right) , \quad (8)$$

where  $\Gamma_{\Delta^+} \simeq 120$  MeV,  $m_{\Delta^+} = 1232$  MeV and  $\sigma_{\Delta^+} \simeq 420 \mu\text{b}$  and  $\langle x_{p \rightarrow \Delta^+} \rangle \simeq 0.2$ . Hence, for a spectral slope  $\alpha \simeq -1$  the optical depth becomes constant above a proton energy

$$E_{p,b} \simeq 0.4 \frac{\Gamma_i^2}{\epsilon_0} \text{ GeV}^2 \simeq 4 \times 10^{16} \frac{\Gamma_{i,2.5}^2}{\epsilon_{0,6}} \text{ eV} , \quad (9)$$

with  $\epsilon_0 = \epsilon_{0,6}$  MeV. Photo-pion production therefore introduces a break in the neutron production spectrum at (9). Above this energy the energy loss length in the comoving frame is

$$t'_\Delta \simeq 4 \times 10^{12} \left( \frac{\epsilon_{0,6} \Gamma_{i,2.5}^5 t_{v,-2}^2}{L_{\gamma,52}} \right) \text{ cm} , \quad (10)$$

and the maximal proton energy satisfying  $t'_\Delta = t'_{\text{acc}}$  is

$$E_{p,\text{max}} \simeq 2 \times 10^{22} \left( \frac{\varepsilon_{B,-1} \Gamma_{i,2.5}^6 t_{v,-2}^2}{\eta^2 \varepsilon_{e,-1} L_{\gamma,52}} \right)^{1/2} \text{ eV} . \quad (11)$$

For GRB fireball parameters considered in this work the scale of photo-pion losses (10) is always larger than the synchrotron scale (6) or the dynamical scale (4). The maximal proton energy is hence given by the smaller of Eqs. (5) and (7).

There is an additional consideration as mentioned in the introduction: because protons are magnetically coupled to the expanding fireball they will lose energy adiabatically if they remain confined in the expanding shock. Adiabatic cooling, however, is not important for neutrons that are produced at scales  $\langle x_{p \rightarrow \Delta} \rangle t'_\Delta$  and can escape the source [13].

We will assume that the spectrum of observable CRs results from neutrons escaping the source. The competition between various energy loss mechanisms in internal shocks can introduce various features in the injection spectrum of individual GRBs [29]. Within our approximation of a homogeneous source distribution we assume that the *effective* CR emission rate can be approximated as

$$Q_{\text{CR}}(E) \simeq Q_0 \frac{(E/E_{p,b})^{-\gamma}}{1 + (E/E_{p,b})^{\beta-\alpha}} e^{-E/E_{p,\text{max}}} . \quad (12)$$

For  $E \gg E_{p,b}$ , this reduces to the typical  $Q_0 E^{-\gamma} \exp(-E/E_{p,\max})$  approximation of the CR injection spectrum that we are going to test against HiRes data in the following. If energy loss of pions and muons prior to decay were negligible, we can relate the neutrino (per flavor) and CR neutron emission rates as

$$Q_\nu^0(E_\nu) \simeq \frac{1}{\epsilon} Q_{\text{CR}}(E_\nu/\epsilon), \quad (13)$$

where  $\epsilon = \langle E_\nu/E_n \rangle \simeq 0.06$ . However, synchrotron losses of secondary pions and muons in the background magnetic field are important. With muon and pion lifetimes of  $t_\mu^{\text{dec}} = 2.2 \mu\text{s}$  and  $t_\pi^{\text{dec}} = 26 \text{ ns}$ , respectively, this will introduce a synchrotron break in the respective spectrum at

$$E'_{\pi/\mu,s} = \frac{3}{4} \sqrt{\frac{m_{\pi/\mu}^5}{\pi \alpha^2 B'^2 t_{\pi/\mu}^{\text{dec}}}} \quad (14)$$

The corresponding break in the neutrino spectra from  $\pi^+ \rightarrow \mu^+ \nu_\mu$  and  $\mu^+ \rightarrow e^+ \bar{\nu}_\mu \nu_e$ , respectively, is  $E'_{\nu,s} \simeq E'_{\pi/\mu,s}/4$  or

$$E_{\nu,s} = \left( \frac{\varepsilon_{e,-1} \Gamma_{i,2.5}^8 t_{v,-2}^2}{\varepsilon_{B,-1} L_{\gamma,52}} \right)^{1/2} \times \begin{cases} 2 \times 10^{17} \text{ eV} & (\nu_\mu), \\ 1 \times 10^{16} \text{ eV} & (\bar{\nu}_\mu, \nu_e). \end{cases} \quad (15)$$

The total diffuse neutrino flux can hence be approximated as

$$Q_{\text{all } \nu}(E_\nu) = \sum_\alpha \frac{Q_\nu^0(E_\nu)}{1 + (E_\nu/E_{\nu\alpha,s})^2}, \quad (16)$$

where the sum runs over the neutrino flavors  $\nu_\alpha = \nu_\mu, \bar{\nu}_\mu$  or  $\nu_e$ .

#### 4. Diffuse Cosmic Spectra

For the calculation of the spectrum of UHE CR protons we assume that the cosmic source distribution is spatially homogeneous and isotropic. The comoving number density  $Y_i = n_i/(1+z)^3$  of nuclei of type  $i$  is then governed by a set of Boltzmann equations of the form:

$$\dot{Y}_i = \partial_E (H E Y_i) + \partial_E (b_i Y_i) - \Gamma_i Y_i + \sum_j \int dE_j \gamma_{j \rightarrow i} Y_j + \mathcal{L}_i, \quad (17)$$

together with the Friedman-Lemaître equations describing the cosmic expansion rate  $H(z)$  as a function of the redshift  $z$ :  $H^2(z) = H_0^2 [\Omega_m(1+z)^3 + \Omega_\Lambda]$ , normalized to its present value of  $H_0 \sim 70 \text{ km s}^{-1} \text{ Mpc}^{-1}$ , in the usual ‘‘concordance model’’ dominated by a cosmological constant with  $\Omega_\Lambda \sim 0.7$  and a (cold) matter component,  $\Omega_m \sim 0.3$  [30]. The time-dependence of the redshift is  $dz = -dt(1+z)H$ . The first and second term in the r.h.s. of Eq. (17) describe continuous energy losses (CEL) due to red-shift and  $e^+e^-$  pair production [31] on the cosmic photon backgrounds, respectively. The third and fourth terms describe more general interactions involving particle losses ( $i \rightarrow$  anything) with interaction rate  $\Gamma_i$ , and particle generation  $j \rightarrow i$ . We use the Monte Carlo package SOPHIA [32] to calculate  $p\gamma$  interaction rates and spectra. The last term,  $\mathcal{L}_i$ , accounts for the CR emission rate per co-moving volume.

We describe the cosmic evolution of the CR sources by the ansatz  $\mathcal{L}_{\text{CR}}(z, E) = \mathcal{H}_{\text{GRB}}(z) Q_{\text{CR}}(E)$ . Given their supernova association it is natural to assume that the comoving density of GRBs follows the star formation rate (SFR). We will use in the following the approximation [33, 34]

$$\mathcal{H}_{\text{SFR}}(z) = \begin{cases} (1+z)^{3.4} & z < 1, \\ N_1 (1+z)^{-0.3} & 1 < z < 4, \\ N_1 N_4 (1+z)^{-3.5} & z > 4, \end{cases} \quad (18)$$

with normalization factors,  $N_1 = 2^{3.7}$  and  $N_4 = 5^{3.2}$ . It has been suggested that the GRB population may not directly follow the SFR and may have been stronger in the past. This possibility is interesting also in the context of UHE CR models: a strong evolution of CR proton sources can account for the spectrum of extra-galactic UHE CRs even below the ankle [35]. These “low-crossover” models predict significantly larger neutrino fluxes from the sources of CR protons and are already limited by upper bounds on diffuse neutrino fluxes [36, 37]. For the illustration of the effect of a strong GRB rate at high redshift we will use in the following a comparatively strong evolution of the from [38]

$$\mathcal{H}_{\text{strong}}(z) = (1+z)^{1.4} \mathcal{H}_{\text{SFR}}(z). \quad (19)$$

This is consistent with a more recent study [39]. However, the sample of high-redshift GRBs where the enhanced evolution (19) becomes strongest is small and plagued by systematics. It has also been argued that the evolution at low redshift is consistent with the SFR whereas at high redshift it can be approximated as an almost constant rate [40–42].

The density of CR sources at high redshift has two effects on the analysis. Firstly, a stronger evolution of the CR sources requires in general lower values of the power-law index  $\gamma$  to reproduce the CR data. Secondly, a higher density of sources in the past tend to produce larger energy densities of secondary neutrinos and  $\gamma$ -rays. However, we will see later on that the contribution of UHE CR proton sources to the diffuse extra-galactic  $\gamma$ -ray background is already close to maximal if we assume a source evolution following the SFR. A stronger evolution as in Eq. (19) can not significantly enhance the prompt neutrino fluxes without violating the  $\gamma$ -ray bound. We will estimate the effect of source evolution on the bolometric electro-magnetic energy density in the following.

Particles with electromagnetic (EM) interactions produced in association with the cosmic rays,  $\gamma$ -rays, electrons and positrons, will cascade in the universal photon background and magnetic fields on time-scales much shorter than their production rates. The relevant processes with background photons are inverse Compton scattering (ICS),  $e^\pm + \gamma_{\text{bgr}} \rightarrow e^\pm + \gamma$ , pair production (PP),  $\gamma + \gamma_{\text{bgr}} \rightarrow e^+ + e^-$ , double pair production (DPP)  $\gamma + \gamma_{\text{bgr}} \rightarrow e^+ + e^- + e^+ + e^-$ , and triple pair production (TPP),  $e^\pm + \gamma_{\text{bgr}} \rightarrow e^\pm + e^+ + e^-$  [31, 43]. High energy electrons and positrons can also lose energy via synchrotron radiation on the intergalactic magnetic field with strength limited to be  $\sim 10^{-9}\text{G}$  [44].

The evolution of the diffuse  $\gamma$ -ray and  $e^\pm$  spectra follows the Boltzmann equations (17). For recent studies see [45, 46]. After cascading the EM flux accumulates into  $\gamma$ -rays of GeV-TeV energy with a characteristic and essentially universal spectrum. Its normalization is determined by the total energy density of EM radiation from the propagation loss of CR nuclei. For this purpose, we define the comoving energy density at redshift  $z$  as

$$\omega_{\text{cas}}(z) \equiv \int dE E \sum_{i=\gamma, e^\pm} Y_i(z, E), \quad (20)$$

which follows the evolution equation

$$\dot{\omega}_{\text{cas}} + H\omega_{\text{cas}} = \int dE b(z, E) Y_{\text{CR}}(z, E). \quad (21)$$

The energy loss rate  $b \equiv dE/dt$  was already defined by Eq. (17), but here comprises the combined energy loss of CR protons into EM radiation by Bethe-Heitler production and photo-pion interactions. The energy density ( $\text{eV cm}^{-3}$ ) of the electromagnetic background observed today is therefore given by

$$\omega_{\text{cas}} = \int dt \int dE \frac{b(z, E)}{(1+z)} Y_{\text{CR}}(z, E). \quad (22)$$

Typically the energy density (20) today obtained by a detailed calculation of the EM spectra agrees with the (quicker) bolometric calculation (22) within a few percent and we will use the latter in our statistical analysis.

The influence of cosmic evolution on the energy density of the cascade can be estimated in the following way. The UHE CR interactions with background photons are rapid compared to cosmic time-scales. The

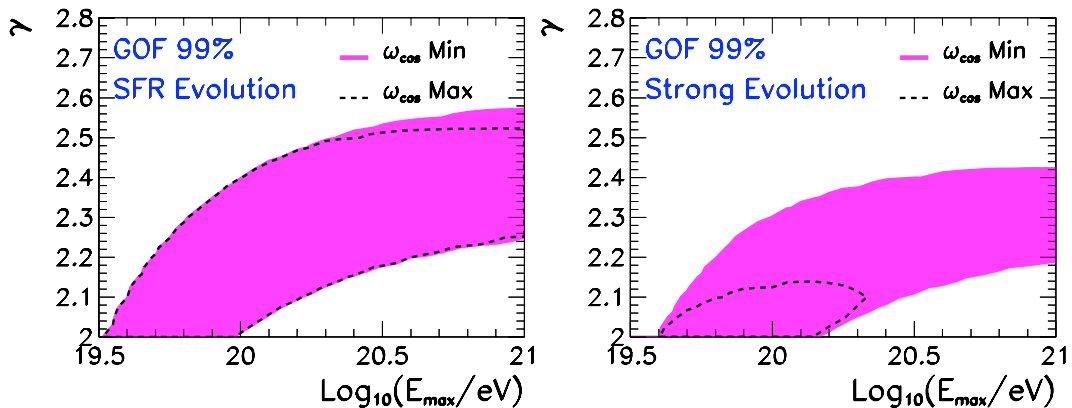


Figure 1: Results of the goodness of fit test of the HiRes data [48]. We show the 99% (magenta) confidence levels of the injection index  $\gamma$  and the maximal energy  $E_{\max}$ . In this analysis we consider only minimal  $\gamma$ -ray production coming from Bethe-Heitler pair production and photo-pion production of CR protons during propagation (“Min”). The dashed line (“Max”) assumes that also  $\gamma$ -rays from  $\pi^0$  production survive the internal shock environment and cascade during propagation in the inter-galactic background.

energy threshold of these processes scales with redshift as  $E_{\text{th}}/(1+z)$  where  $E_{\text{th}}$  is the (effective) threshold today. We can therefore approximate the evolution of the energy density of the secondaries as

$$\dot{\omega}_{\text{cas}} + H\omega_{\text{cas}} \simeq \eta_{\text{cas}} \mathcal{H}(z) \int_{E_{\text{th}}/(1+z)} dE E Q_{\text{CR}}(E), \quad (23)$$

where  $\eta_{\text{cas}}$  denotes the energy fraction of the CR luminosity converted to the electromagnetic cascade. Assuming a power-law injection  $Q_{\text{CR}}(E) \propto E^{-\gamma}$  with sufficiently large cutoff  $E_{\max} \gg E_{\text{th}}$  we obtain that strong cosmic evolution (19) enhances the diffuse  $\gamma$ -spectrum as  $\omega_{\text{cas}} \propto \int dt (1+z)^{1.4+\gamma-2}$ . For the proton spectrum  $\gamma \simeq 2.3$  this corresponds to a relative increase of  $\sim 4$ , which agrees with numerical results.

Photo-hadronic interactions in internal shocks produce EM radiation from the decay of pions. Most of this additional EM radiation is expected to cascade in the high background densities of  $\gamma$ -rays or  $e^\pm$  and strong magnetic fields of the fireball and should eventually contribute to the luminosity of the burst. However, it is conceivable that part of it decouples from the fireball to contribute an additional source term  $Q_{\text{EM}}$  [47] to the diffuse  $\gamma$ -ray background. Assuming energy conservation in the cascade this additional contribution is smaller than

$$\omega_{\text{cas,source}} = \frac{\xi}{H_0} \int dE E Q_{\text{EM}}(E) \quad (24)$$

with  $\xi/H_0 \equiv \int dt \mathcal{H}(z)/(1+z)$ . Assuming the GRB evolution (18) and (19) this gives  $\xi_{\text{SFR}} \simeq 2.4$  and  $\xi_{\text{strong}} \simeq 7.3$ , respectively.

In the following we will assume two limiting cases for the contribution of GRBs to the diffuse GeV-TeV background. The minimal model (“Min”) assumes that the only contribution to the cascade results from the propagation from CR protons. In a maximal model (“Max”) we assume that additionally all  $\gamma$ -rays from neutral pion production in the GRB contribute maximally to the cascade in the form of the term (24) with  $Q_{\text{EM}} = Q_{\pi^0}$ .

## 5. Goodness of Fit Test

In this section we present the details and results of our statistical analysis. We perform a goodness of fit (GOF) test of the compatibility of cosmic ray data with a given model, characterized by the spectral index  $\gamma$  and the maximal energy  $E_{\max}$  of the injected cosmic ray and by the two evolution models (18) and (19). We use CR data from HiRes I and II [48] above the “ankle” at 4 EeV. We additionally impose the

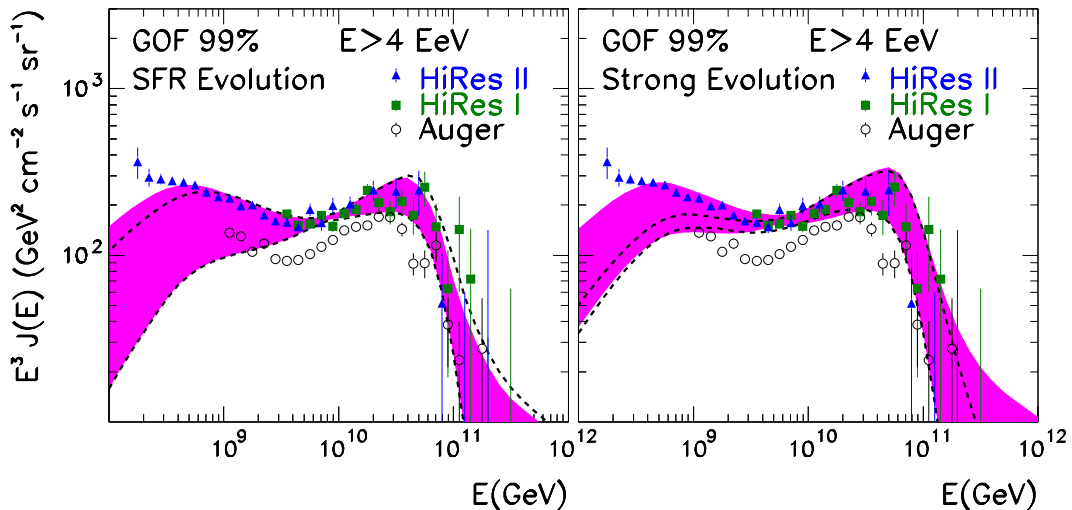


Figure 2: The allowed proton range of proton flux at the 99% confidence level. The color-coding is as in Fig. 1. Each fit of the proton spectrum is marginalized with respect to the experimental energy uncertainty and we show the shifted predictions in comparison to the HiRes central values [48]. For comparison we also show the Auger data [50] which has *not* been included in the fit.

requirement that the electromagnetic flux accompanying the cosmic rays does not exceed the Fermi-LAT measurements of the diffuse extra-galactic  $\gamma$ -ray background in the GeV-TeV energy range.

Given the acceptance  $A_i$  (in units of area per unit time per unit solid angle) of the experiment in bin  $i$  centered at energy  $E_i$  with bin width  $\Delta_i$  and energy scale uncertainty  $\sigma_{E_s}$ , the number of events expected in the bin is

$$N_i(\gamma, E_{\max}, \mathcal{N}, \delta) = A_i \int_{E_i(1+\delta)-\Delta_i/2}^{E_i(1+\delta)+\Delta_i/2} dE J_{\mathcal{N}, \gamma, E_{\max}}^p(E), \quad (25)$$

where  $J_{\mathcal{N}, \gamma, E_{\max}}^p(E) = n_p(0, E)/4\pi$  is the proton flux arriving at the detector. It is determined by the source luminosity of Eq. (12) with  $E_{p,b} \ll E_{\min} = 4$  EeV and cosmic evolution given by Eqs. (18) or (19). The parameter  $\delta$  in Eq. (25) is a fractional energy-scale shift that takes into account the uncertainty in the energy-scale and  $\mathcal{N}$  is the normalization of the proton source luminosity.

The probability distribution of events in the  $i$ -th bin follows a Poisson distribution with mean  $N_i$ . Correspondingly, the  $r$ -dimensional probability distribution for a set of non-negative integer numbers  $\vec{k} = \{k_1, \dots, k_r\}$ ,  $P_{\vec{k}}(n, \gamma, \mathcal{N}, \delta)$  is just the product of the individual Poisson distributions with  $r$  the number of bins with  $E_i \geq E_{\min}$ . Given a model, the experimental result  $\vec{N}^{\text{exp}} = \{N_1^{\text{exp}}, \dots, N_r^{\text{exp}}\}$  has a probability  $P_{\vec{N}^{\text{exp}}}(\gamma, E_{\max}, \mathcal{N}, \delta)$  which, after marginalizing over the uncertainty in the energy scale and normalization, is given by

$$P_{\text{exp}}(\gamma, E_{\max}) = \max_{\delta, \mathcal{N}} (P_{\vec{N}^{\text{exp}}}(\gamma, E_{\max}, \mathcal{N}, \delta)). \quad (26)$$

Here the maximization is for some prior for  $\delta$  and  $\mathcal{N}$ . As a prior the energy shift  $\delta$  we used a top hat of width  $\sigma_{E_s}$ .

For  $\mathcal{N}$  we impose two priors. The first is associated with the upper bound on the total EM of Eq. (22) that should not exceed the Fermi-LAT measurements [27], or following Ref. [45]

$$w_{\text{cas}}(\mathcal{N}, \gamma, E_{\max}) \leq 5.8 \times 10^{-7} \text{ eV/cm}^3. \quad (27)$$

The second prior on the normalization is imposed by requiring that the proton spectra do not exceed the HiRes I and II data below  $E_{\min}$  by more than three standard deviations.



The marginalization in Eq. (26) also determines  $\mathcal{N}_{\text{best}}$  and  $\delta_{\text{best}}$  for the model, which are the values of the energy shift and normalization that yield the best description of the experimental CR data, subject to the constraint imposed by the Fermi-LAT measurement.

In the end the model is compatible with the experimental results at a given GOF if

$$\sum_{P_{\bar{k}} > P_{\text{exp}}} P_{\bar{k}}(\gamma, E_{\text{max}}, \mathcal{N}_{\text{best}}, \delta_{\text{best}}) \leq \text{GOF}. \quad (28)$$

Technically, this calculation is performed by generating a large number  $N_{\text{rep}}$  of replica experiments following the probability distribution  $P_{\bar{k}}$  and by imposing that the fraction  $F$  with  $P_{\bar{k}} > P_{\text{exp}}$  satisfy  $F \leq \text{GOF}$ .

With this method we determine the range of values of  $(\gamma, E_{\text{max}})$  that are compatible with the HiRes I and HiRes II data [48]. We show in Fig. 1 the regions with GOF 99% for the two evolution models (18) (left panel) and (19) (right panel). In order to illustrate the impact of the constraint imposed by the Fermi-LAT measurements, we also show the GOF regions without imposing it. The region bounded by the dotted line shows the reduced parameter space resulting from the condition that secondary EM radiation from proton propagation does not exceed the Fermi-LAT measurement (“Min”). This bound can become even stronger if we consider UHE  $\gamma$ -ray emission from  $\pi^0$  decay in the source with diffuse energy density (24) as indicated by the region bounded by the dashed line (“Max”). Figure 2 shows the range of the corresponding proton fits to the data.

We have not included in the analysis the results from the Auger Collaboration [49, 50], which are shown in Fig.2 for illustration only. As described in Refs. [49, 50], besides the energy scale uncertainty there is also an (energy-dependent) energy resolution uncertainty which implies that bin-to-bin migrations influence the reconstruction of the flux and spectral shape. Since the form of the corresponding error matrix is not public, this data [49, 50] cannot be analysed outside the Auger Collaboration.

## 6. Results and Their Dependence on Model Parameters

Our final results are summarized in Fig. 3 that shows the range of prompt neutrino spectra corresponding to the UHE CR proton spectra at the 99% C.L. of the GOF test with the HiRes data assuming SFR evolution (left panels) and the stronger evolution of Eq. (19) (right panels). We have assumed that proton acceleration in the shocks is efficient ( $\eta \simeq 1$ ) and have fixed the maximum  $\epsilon_0$  of the prompt  $\gamma$ -ray emission (Eq. (2)) at 1 MeV. For each GRB model the maximum proton energy  $E_{\text{max}}$  corresponds to the smaller of Eq. (5) or (7), *i.e.*  $t_{\text{dyn}} < t_{\text{syn}}$  or  $t_{\text{syn}} < t_{\text{dyn}}$ , respectively. For given values of  $E_{\text{max}}$ ,  $\Gamma_i$  and  $t_v$  we can in general derive two solutions of  $(\epsilon_B/\epsilon_e)L_\gamma$ , which we allow to vary within the range  $0.1 < (\epsilon_B/\epsilon_e)L_{\gamma,52} < 10$ . The corresponding branches are indicated in the plots.

The upper three rows of Fig. 3 shows prompt neutrino spectra with a Doppler factor  $\Gamma_i = 10^{2.5}$  of the internal shock. The top panels show the results for the variation time-scale  $t_v = 0.01$ . This includes the range of neutrino fluxes for typical “benchmark” values of the GRB environment with  $L_\gamma = 10^{52}$  erg/s and  $E_{\text{max}} = 10^{20.5}$  eV, which is shown separately as the cross-hatched area. The range of prompt neutrino spectra for the benchmark model corresponds to the range of the power-law index  $\gamma$  at the 99% C.L. and the normalization of each particular model. Note, that for both cases, SFR or strong evolution, the range of the prompt neutrino flux exceeds the present limits of IC-40.

The energy density of the prompt neutrino spectrum peaks at an energy  $E \simeq \epsilon E_{p,b} \simeq 1$  PeV and is marginally consistent with recent upper limits on the diffuse neutrino flux by IC-40 [51, 52]. Only for very short variation time-scales of  $t_v \simeq 10^{-3}$  s (third row of Fig. 3) and for synchrotron-loss-dominated GRBs ( $t_{\text{syn}} < t_{\text{dyn}}$ ) can the predicted flux avoid present upper limits. Note that since  $E_{p,b} \propto \Gamma_i^2/\epsilon_0$  we can shift the peak to higher energies assuming a stronger Doppler boost of the internal shocks. However, the condition  $E_{p,b} \lesssim E_{\text{min}}$  imposed for the fit requires that  $\Gamma_i \lesssim 10^{3.5}$  and hence  $\epsilon E_{p,b} \lesssim 100$  PeV.

The bottom row of Fig. 3 we show the prompt neutrino spectra for  $\Gamma_i = 10^3$  and the full range of variability  $10^{-3} < t_v/s < 0.1$ . Due to the strong dependence of the synchrotron time scale on the Doppler factor,  $t'_{\text{syn}} \propto \Gamma_i^7$ , the GRB models at the 99% C.L. correspond to proton sources where the maximal energy is limited by the dynamical time. The range of the flux is consistent with present IC-40 limits. Note,

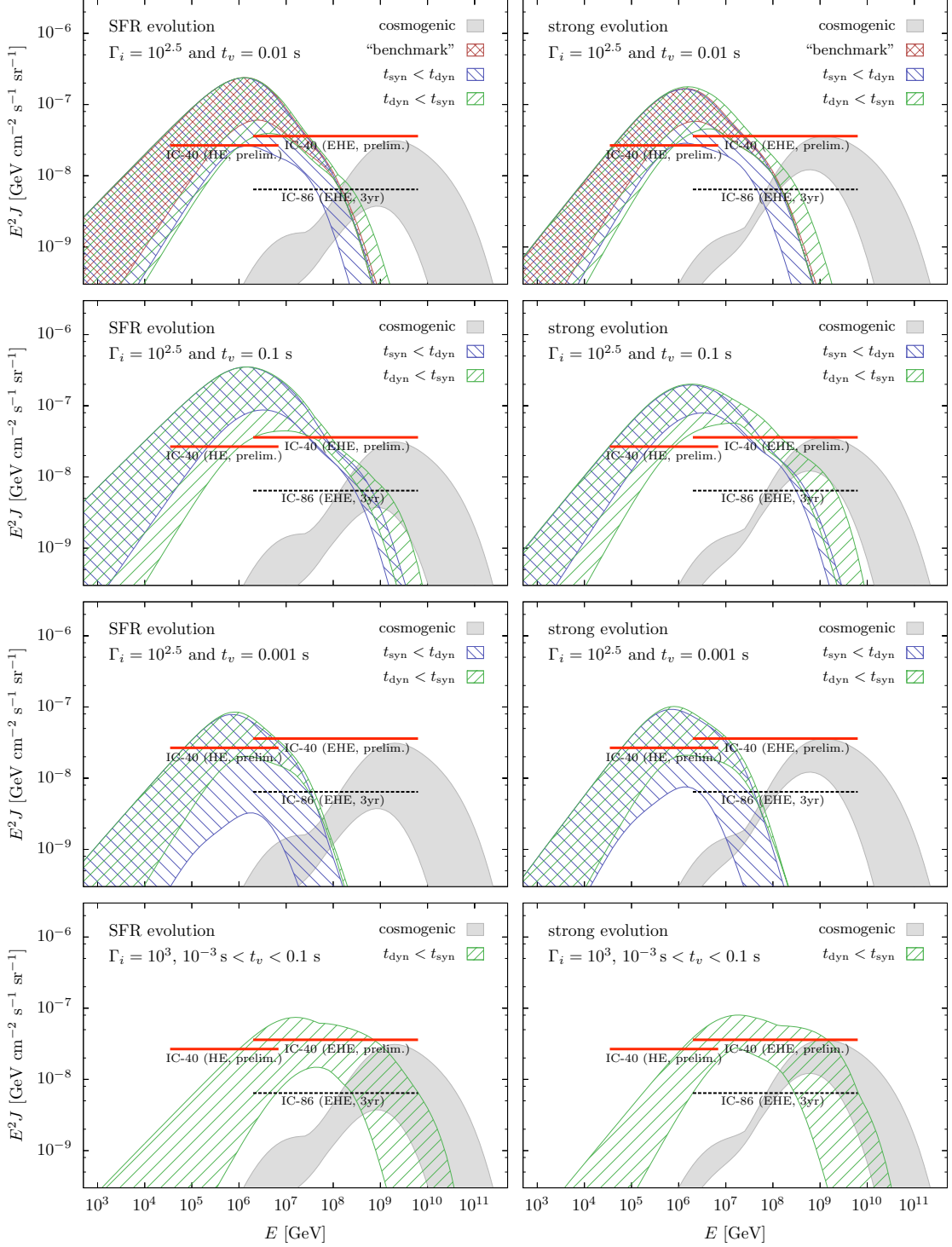


Figure 3: Prompt neutrino spectra for SFR (left) and strong (right) evolution corresponding to the 99% C.L. of the “Min” model shown in Fig. 1 and assuming the luminosity range  $0.1 < (\varepsilon_B/\varepsilon_e)L_{\gamma,52} < 10$ . We show the prompt spectra separately for the branches  $t_{\text{dyn}} < t_{\text{syn}}$  (green right-hatched) and  $t_{\text{syn}} < t_{\text{dyn}}$  (blue left-hatched). The preliminary IceCube limits [51, 52] (90% C.L.) on the total neutrino flux from the analysis of high-energy (HE) and extremely-high energy (EHE) neutrinos with the 40 string sub-array (IC-40) assume 1:1:1 flavor composition after oscillation. We also show the sensitivity of the full IceCube detector (IC-86) to EHE neutrinos after three years of observation. The gray solid area shows the range of GZK neutrinos expected at the 99% C.L.

however, that the opacity of the GRBs for UHE  $p\gamma$  interactions and subsequent emission of CR neutrons is very sensitive to the Doppler factor,

$$\tau_{p\gamma} \simeq \frac{t'_{\text{dyn}}}{t'_{\Delta} \langle x_{p \rightarrow \Delta} \rangle} \simeq 0.1 \left( \frac{L_{\gamma,52}}{\Gamma_{i,2.5}^4 t_{v,-2\epsilon 0,6}} \right). \quad (29)$$

Increasing the average Doppler factor of the GRB from  $10^{2.5}$  to  $10^3$  reduces the efficiency of UHE CR emission by two orders of magnitude. It is hence more likely that the successful candidates of CR sources are GRBs with lower  $\Gamma_i$ .

The range of prompt neutrino spectra shown in Fig. 3 spans about two orders of magnitude, a range larger than a previous study in Ref. [53]. The difference of the results can be traced back to different assumptions. Firstly, we here assumed that only neutrons can escape the GRB shock environment and form the spectrum of UHE CRs. Hence, both, CR and neutrino spectra depend on the opacity of the source. Secondly, we apply a statistical fit to the data assuming a wide range of spectral indices. Statistically allowed CR spectra with a steep injection index  $\gamma \gg 2$  correspond to GRB models with a higher bolometric energy density and hence larger prompt neutrino emission. For large maximal proton energies,  $E_{\text{max}} \gg 10^{19}$  eV, we can approximate the total local power density in UHE CRs derived from the best fit to the HiRes data as

$$\dot{\epsilon}_{\text{CR}} \equiv \int_{E_{p,b}} dE E \mathcal{L}_{\text{CR}}(0, E) \simeq (1-2) \times 10^{44} \text{ erg Mpc}^{-3} \text{ yr}^{-1} \times \begin{cases} \frac{1}{\gamma-2} \left( \frac{10^{19} \text{ eV}}{E_{p,b}} \right)^{\gamma-2} & \gamma > 2, \\ \ln \left( \frac{E_{\text{max}}}{E_{p,b}} \right) & \gamma = 2. \end{cases} \quad (30)$$

This value is consistent with the original study by Waxman and Bahcall [15] assuming a total power density in UHE CRs of the order of  $4 \times 10^{44} \text{ erg Mpc}^{-3} \text{ yr}^{-1}$  between  $10^{19}$  eV and  $10^{21}$  eV assuming a flat spectrum with power-law index  $\gamma = 2$ . In our approach we allow steeper injection spectra  $\gamma \gg 2$  extending down to the break energy  $E_{p,b} \ll 10^{19}$  eV (cf. Eq. (9)) which is set by the GRB fireball environment. For very steep injection spectra with  $\gamma \simeq 2.6$  consistent with our fit at the 99% C.L. (cf. left panel in Fig. 1) and  $E_{p,b} = 4 \times 10^{16}$  eV this corresponds to a maximal local power density of the order of  $\dot{\epsilon}_{\text{CR,max}} \simeq 10^{46} \text{ erg Mpc}^{-3} \text{ yr}^{-1}$ .

These large local power densities of steep UHE CR proton spectra are also consistent with the results of Ref. [54]. In contrast to Ref. [54] we include here the limits implied by the extra-galactic diffuse  $\gamma$ -ray background inferred by Fermi LAT. This bound has the strongest effect on strong evolution models with large power-law index as can be seen in the right panel of Fig. 1. The corresponding proton fluxes at the 99% C.L. are shown in the right panels of Fig. 2 and the prompt neutrino fluxes in the right panels of Fig. 3. The range of spectra is comparable to the moderate evolution following SFR (left panels) since the contribution of UHE CRs to the diffuse extra-galactic  $\gamma$ -ray background is already close to maximal.

## 7. Conclusion

We have discussed prompt neutrino emission associated with the production of UHE CR protons in GRBs. Our analysis assumes that UHE CRs above the ‘‘ankle’’ at 4 EeV consists of neutrons emitted from  $p\gamma$  interactions in internal shocks of the GRB fireball model. We determined the CR emission density by a fit to HiRes data and used this information to determine the corresponding neutrino fluxes for a wide range of parameters for the shock environment. We have also carefully studied the effect of secondary production during CR propagation in the form of GZK neutrinos as well as the GeV-TeV  $\gamma$ -ray background.

The main results are shown in Fig. 3. We have shown that typical (‘‘benchmark’’) fireball environments predict prompt neutrino fluxes that exceed present diffuse neutrino limits from IceCube (IC-40) if the associated proton spectrum is fitted to actual CR data. This remains partially true if we relax the condition of internal shock parameters. Consistency with the diffuse neutrino limits requires that the CR acceleration takes place in GRB fireballs with small internal shock radii (corresponding to variation time-scales of milliseconds) and/or large Lorentz boost  $\Gamma_i \simeq 1000$ . Alternatively, it is possible that UHE CRs at the ankle might still receive a significant contribution from galactic CRs, which lowers the required power density in extra-galactic CRs and the corresponding prompt neutrino spectra from GRB sources [55]. However, one

has to worry that galactic CRs at these energies will reveal themselves via an anisotropy toward the galactic center. In any case, the sensitivity of the full IceCube observatory (IC-86) after three years of observation will improve present diffuse neutrino limits by a factor five and will serve as a crucial test of the GRB scenario of UHE CRs.

Finally, we would also like to mention additional constraints of this CR scenario. A fraction of UHE  $\gamma$ -rays produced in neutral pion production may escape the fireball shocks and contribute to the GeV-TeV background as well. As an estimate, we have tested a pessimistic scenario (“Max” model) where all  $\gamma$ -rays from  $\pi^0$  production escape the source. We found that this additional contribution may become important in the case of source evolution much stronger than the SFR (*cf.* dashed regions in Figs. 1 and 2). It is also possible to constrain UHE CR emission from internal shocks of GRBs by the integrated fluence of all bursts as has been done recently in [56]. On the other hand, the contribution of the burst spectrum to the diffuse  $\gamma$ -ray background from unidentified cosmic GRBs has been discussed in [57] and has been shown to contribute a relatively small fraction.

## Acknowledgments

The authors would like to thank Peter Meszaros, Kohta Murase, Eli Waxman and Walter Winter for valuable comments on the manuscript. This work is supported by US National Science Foundation Grant No PHY-0969739 and by the Research Foundation of SUNY at Stony Brook. F.H. is supported by U.S. National Science Foundation-Office of Polar Program, U.S. National Science Foundation-Physics Division, and the University of Wisconsin Alumni Research Foundation. M.C.G-G acknowledges further support from Spanish MICCIN grants 2007-66665-C02-01, consolider-ingenio 2010 grant CSD2008-0037 and by CUR Generalitat de Catalunya grant 2009SGR502.

## References

- [1] A. Shemi and T. Piran, *Astrophys. J.* **365**, L55 (1990).
- [2] M. J. Rees and P. Meszaros, *Mon. Not. Roy. Astron. Soc.* **258**, 41 (1992).
- [3] P. Meszaros and M. J. Rees, *Astrophys. J.* **405**, 278 (1993).
- [4] M. J. Rees and P. Meszaros, *Astrophys. J.* **430**, L93 (1994) [arXiv:astro-ph/9404038].
- [5] B. Paczynski and G. H. Xu, *Astrophys. J.* **427**, 708 (1994).
- [6] P. Meszaros, M. J. Rees and H. Papatthanassiou, *Astrophys. J.* **432**, 181 (1994) [arXiv:astro-ph/9311071].
- [7] P. Meszaros and M. J. Rees, *Mon. Not. Roy. Astron. Soc.* **269**, L41 (1994) [arXiv:astro-ph/9404056].
- [8] P. Meszaros, *Rept. Prog. Phys.* **69**, 2259 (2006) [arXiv:astro-ph/0605208].
- [9] B. D. Metzger, D. Giannios and S. Horiuchi, arXiv:1101.4019 [astro-ph.HE].
- [10] R. U. Abbasi *et al.* [HiRes Collaboration], *Phys. Rev. Lett.* **104**, 161101 (2010). [arXiv:0910.4184 [astro-ph.HE]].
- [11] J. Abraham *et al.* [Pierre Auger Collaboration], *Phys. Rev. Lett.* **104**, 091101 (2010). [arXiv:1002.0699 [astro-ph.HE]].
- [12] R. Ulrich, R. Engel, S. Muller, F. Schussler and M. Unger, *Nucl. Phys. Proc. Suppl.* **196**, 335 (2009) [arXiv:0906.3075 [astro-ph.HE]].
- [13] J. P. Rachen and P. Meszaros, *AIP Conf. Proc.* **428**, 776 (1997) [arXiv:astro-ph/9811266].
- [14] J. P. Rachen and P. Meszaros, *Phys. Rev. D* **58**, 123005 (1998) [arXiv:astro-ph/9802280].
- [15] E. Waxman and J. N. Bahcall, *Phys. Rev. Lett.* **78**, 2292 (1997) [arXiv:astro-ph/9701231].
- [16] J. N. Bahcall and E. Waxman, *Phys. Rev. D* **64**, 023002 (2001) [arXiv:hep-ph/9902383].
- [17] K. Murase and S. Nagataki, *Phys. Rev. D* **73**, 063002 (2006) [arXiv:astro-ph/0512275].
- [18] L. A. Anchordoqui, D. Hooper, S. Sarkar and A. M. Taylor, *Astropart. Phys.* **29**, 1 (2008) [arXiv:astro-ph/0703001].
- [19] J. Ahrens *et al.* [IceCube Collaboration], *Astropart. Phys.* **20**, 507 (2004) [arXiv:astro-ph/0305196].
- [20] R. Abbasi *et al.* [IceCube Collaboration], *Phys. Rev. Lett.* **106**, 141101 (2011) [arXiv:1101.1448 [astro-ph.HE]].
- [21] S. Razzaque, P. Meszaros and E. Waxman, *Phys. Rev. Lett.* **90**, 241103 (2003) [arXiv:astro-ph/0212536].
- [22] K. Murase and S. Nagataki, *Phys. Rev. Lett.* **97**, 051101 (2006) [arXiv:astro-ph/0604437].
- [23] K. Murase, *Phys. Rev. D* **76**, 123001 (2007) [arXiv:0707.1140 [astro-ph]].
- [24] S. Razzaque, O. Mena and C. D. Dermer, *Astrophys. J.* **691**, L37 (2009).
- [25] K. Greisen, *Phys. Rev. Lett.* **16**, 748 (1966).
- [26] G. T. Zatsepin and V. A. Kuzmin, *JETP Lett.* **4**, 78 (1966) [*Pisma Zh. Eksp. Teor. Fiz.* **4**, 114 (1966)].
- [27] A. A. Abdo *et al.* [Fermi-LAT Collaboration], *Phys. Rev. Lett.* **104**, 101101 (2010) [arXiv:1002.3603 [astro-ph.HE]].
- [28] D. Band *et al.*, *Astrophys. J.* **413**, 281 (1993).
- [29] R. J. Protheroe and T. Stanev, *Astropart. Phys.* **10**, 185 (1999) [arXiv:astro-ph/9808129].
- [30] K. Nakamura *et al.* [Particle Data Group], *J. Phys. G* **37**, 075021 (2010).
- [31] G. R. Blumenthal, *Phys. Rev. D* **1**, 1596 (1970).

- [32] A. Mucke, R. Engel, J. P. Rachen, R. J. Protheroe and T. Stanev, *Comput. Phys. Commun.* **124**, 290 (2000) [arXiv:astro-ph/9903478].
- [33] A. M. Hopkins and J. F. Beacom, *Astrophys. J.* **651**, 142 (2006) [arXiv:astro-ph/0601463].
- [34] H. Yuksel, M. D. Kistler, J. F. Beacom and A. M. Hopkins, *Astrophys. J.* **683**, L5 (2008) [arXiv:0804.4008 [astro-ph]].
- [35] V. Berezhinsky, A. Z. Gazizov and S. I. Grigorieva, *Phys. Rev. D* **74**, 043005 (2006) [arXiv:hep-ph/0204357].
- [36] M. Ahlers, L. A. Anchordoqui, H. Goldberg, F. Halzen, A. Ringwald and T. J. Weiler, *Phys. Rev. D* **72**, 023001 (2005) [arXiv:astro-ph/0503229].
- [37] M. Ahlers, L. A. Anchordoqui and S. Sarkar, *Phys. Rev. D* **79**, 083009 (2009) [arXiv:0902.3993 [astro-ph.HE]].
- [38] H. Yuksel and M. D. Kistler, *Phys. Rev. D* **75**, 083004 (2007) [arXiv:astro-ph/0610481].
- [39] M. D. Kistler, H. Yuksel, J. F. Beacom, A. M. Hopkins and J. S. B. Wyithe, *Astrophys. J.* **705**, L104 (2009) [arXiv:0906.0590 [astro-ph.CO]].
- [40] T. Le and C. D. Dermer, *Astrophys. J.* **661**, 394 (2007) [arXiv:astro-ph/0610043].
- [41] D. Guetta and T. Piran, *JCAP* **0707**, 003 (2007) [arXiv:astro-ph/0701194].
- [42] D. Wanderman and T. Piran, *Mon. Not. Roy. Astron. Soc.* **406**, 1944 (2010) [arXiv:0912.0709 [astro-ph.HE]].
- [43] G. R. Blumenthal and R. J. Gould, *Rev. Mod. Phys.* **42**, 237 (1970).
- [44] P. P. Kronberg, *Rept. Prog. Phys.* **57**, 325 (1994).
- [45] V. Berezhinsky, A. Gazizov, M. Kachelriess and S. Ostapchenko, *Phys. Lett. B* **695**, 13 (2011) [arXiv:1003.1496 [astro-ph.HE]].
- [46] M. Ahlers, L. A. Anchordoqui, M. C. Gonzalez-Garcia, F. Halzen and S. Sarkar, *Astropart. Phys.* **34**, 106 (2010) [arXiv:1005.2620 [astro-ph.HE]].
- [47] S. Razzaque, P. Meszaros and B. Zhang, *Astrophys. J.* **613**, 1072 (2004) [arXiv:astro-ph/0404076].
- [48] R. Abbasi *et al.* [HiRes Collaboration], *Phys. Rev. Lett.* **100**, 101101 (2008) [arXiv:astro-ph/0703099].
- [49] J. Abraham *et al.* [Pierre Auger Collaboration], *Phys. Rev. Lett.* **101**, 061101 (2008) [arXiv:0806.4302 [astro-ph]].
- [50] J. Abraham *et al.* [Pierre Auger Collaboration], *Phys. Lett. B* **685**, 239 (2010) [arXiv:1002.1975 [astro-ph.HE]].
- [51] A. Ishihara, *Proceedings of TEXAS 2010*, Heidelberg, Germany.
- [52] R. Abbasi *et al.* [IceCube Collaboration], arXiv:1103.4250 [astro-ph.CO]; arXiv:1104.5187 [astro-ph.HE].
- [53] D. Guetta, M. Spada and E. Waxman, *Astrophys. J.* **559**, 101 (2001) [arXiv:astro-ph/0102487].
- [54] S. D. Wick, C. D. Dermer and A. Atoyan, *Astropart. Phys.* **21**, 125 (2004) [arXiv:astro-ph/0310667].
- [55] B. Katz, R. Budnik and E. Waxman, *JCAP* **0903**, 020 (2009) [arXiv:0811.3759 [astro-ph]].
- [56] D. Eichler, D. Guetta and M. Pohl, *Astrophys. J.* **722**, 543 (2010) [arXiv:1007.3742 [astro-ph.HE]].
- [57] C. D. Dermer, *Astrophys. Space Sci.* **309**, 127 (2007) [arXiv:astro-ph/0610195].